Eur. Phys. J. D **29**, 27–31 (2004)
DOI: 10.1140/epjd/e2004-00003-9

THE EUROPEAN PHYSICAL JOURNAL D

A theoretical study of the Y_3O clusters

Guangyi Gu[1,2], Bing Dai[2], Xunlei Ding[2], and Jinlong Yang[2,a]

[1] Department of Mathematics and Physics, Anhui University of Science and Technology, Huainan, Anhui 232001, P.R. China
[2] Laboratory of Bond Selective Chemistry, University of Science and Technology of China, Hefei, Anhui 230026, P.R. China

Received 25 August 2003 / Received in final form 5 November 2003
Published online 20 January 2004 –

Abstract. Hybrid density functional calculations are performed to study the structural and electronic properties of neutral, anionic and cationic Y_3O clusters. The most stable structures of these clusters are found to be triply bridging oxygen atom structures with C_S symmetry. The ground states of Y_3O, Y_3O^- and Y_3O^+ are doublet ($^2A''$), triplet ($^3A''$) and singlet ($^1A'$), respectively. The calculated electron affinities and ionization potentials are in good agreement with the available experimental data. Time-dependent density functional theory is used to calculate the low-lying excited states. A theoretical assignment for the features in the experimental photoelectron spectra is given.

PACS. 36.40.Mr Spectroscopy and geometrical structure of clusters – 31.15.Ew Density-functional theory – 34.50.Gb Electronic excitation and ionization of molecules; intermediate molecular states (including lifetimes, state mixing, etc.)

1 Introduction

Because of wide applications in many areas, such as high-temperature chemistry, nanotechnology, material science and microelectronics [1–3], transition metal clusters, especially transition metal oxide clusters, have attracted a lot of attention in decades from both theory and experiment. However, our knowledge of transition metal clusters is far from completeness, especially on their excited states. At the same time, the studies about second- or third-row transition metal and transition metal oxide clusters are quite scarce because these clusters have a large number of electrons and electronic states, which makes both spectroscopy studies and theoretical calculations rather difficult.

Photoelectron spectroscopy (PES) is an effective experimental method to study the electronic structure of free molecules and clusters, especially their low-lying excited states. Recently, there are several experimental studies on small yttrium oxide clusters. Knickelbein [4] probed the PES of Y_nO^+ clusters and measured their electron vertical ionization potentials (IP). Wu and Wang [5] have carried out executed vibrationally resolved photodetachment studies on YO_n^- ($n = 1-5$) clusters. Pramann et al. [6] presented the PES of $Y_nO_m^-$, measured the electron affinities and vertical detachment energies, and discussed some of their structures quantitatively.

From a theoretical point of view, time-dependent density functional theory (TDDFT) methodology [7] has been proved not only to be more satisfactory than CI-Single [8], but also to be a reliable method for calculating excitation energies for the open-shell transition metal oxides clusters [9,10]. Recently, Dai et al. [11] made an assignment based on the TDDFT method for the features in the PES of Y_4O^-, and got an excellent agreement with the PES.

In this paper we perform a systematic study on Y_3O in its neutral, anionic and cationic charge states using hybrid density functional theory (DFT) and then calculate the excitation energies to assign the features in the available PES using TDDFT. All the calculated results are in good agreement with the available experimental data.

2 Computational detail

All computations are performed with Gaussian98 [12] programs. The hybrid DFT is used in the ground state calculations and the TDDFT in excited states. Both the ground states of Y_3O, Y_3O^- and Y_3O^+, and the excited states of Y_3O are calculated within unrestricted Kohn-Sham formalism with a three-parameter exchange and correlation functional B3LYP [13]. The standard LANL2DZ in Gaussian98 is employed as the basis set, which has been proved to be suitable for the transition metal systems [9,14]. Geometry optimizations are carried out until the gradient forces vanished with respect to a threshold value of 10^{-6} a.u. All calculations are performed with (75, 302) pruned grid.

[a] e-mail: jlyang@ustc.edu.cn

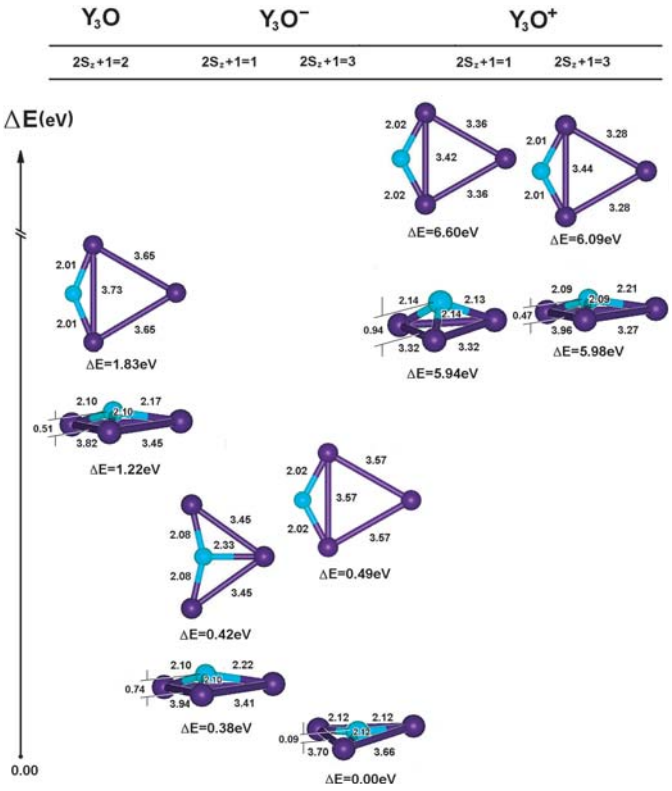

Fig. 1. Structures, bond lengths (Å) and binding energies (relative value in eV) of Y_3O, Y_3O^- and Y_3O^+.

3 Results and discussion

3.1 Geometric and electronic structures of Y_3O, Y_3O^-, Y_3O^+

Pramann et al. [6] presented PES of Y_3O^- and proposed that the geometry structure of Y_3O is most probably a planar C_{2V} structure, very similar as in the case of V_3O, Nb_3O and Ta_3O [15]. This conjecture needs to be verified.

When we optimize the structure of Y_3O^-, several various initial structures are chosen, such as linear structures (straight or bend), planar structures (rhombic or monocyclic, a triangular Y_3 trimer with an oxygen atom at a vertex or with the oxygen inside) and three-dimensional structures. Some of them are transition states with imaginary frequencies. Two stable isomers, a doubly bridging oxygen atom structure with C_{2V} symmetry and a triply bridging oxygen atom structure with C_S symmetry, are found, shown in Figure 1. For both singlets and triplets of Y_3O^-, the total energies of C_{2V} structures are 0.04 eV and 0.49 eV higher than those of C_S structures, respectively. This result contrasts with the suggestion of Pramann et al. [6].

We also check a triply bridging oxygen atom structure with C_{3V} symmetry and found it is not stable. Not only the total energy is a little higher, but also an imaginary frequency exists. When we release the symmetry constraint, this structure is relaxed to the C_S structure. So we confirm that the pyramid with C_S symmetry is the structure of ground state of Y_3O^-. Since both C_{3V} and C_S structures are triplet non-degenerated states, this symmetry break could not be a Jahn-Teller effect.

Table 1. Point group (PG) and harmonic frequencies (cm^{-1}) of the most stable neutral and ionic Y_3O.

system	PG	frequencies (cm^{-1})					
Y_3O	C_S	74	85	122	300	364	512
Y_3O^-	C_S	52	62	117	227	471	477
Y_3O^+	C_S	52	69	137	280	357	555

We consider doublet states for the neutral system and singlet and triplet states for the cationic one. In all cases the total energies of the doubly bridging oxygen atom structures are also higher than those of the triply bridging oxygen atom structures, respectively. So all optimized ground state structures of Y_3O, Y_3O^- and Y_3O^+ are triply bridging oxygen atom structures, and are considerably more stable than the doubly bridging oxygen atom structures.

The ground states of the most stable Y_3O, Y_3O^- and Y_3O^+ isomers are doublet ($^2A''$), triplet ($^3A''$) and singlet ($^1A'$), respectively. Figure 1 shows that all the three ground state structures have the same C_S symmetry.

The vibrational frequencies of the Y_3O, Y_3O^- and Y_3O^+ ground states are listed in Table 1. The absence of imaginary frequency indicates that the triply bridging oxygen atom structures indeed correspond to local minima of the potential energy surface. Because of the minor difference for geometries of the three clusters, there exists only a little difference of vibrational frequencies among them.

The electronic configurations are useful to analyze the electronic transitions. For neutral Y_3O, the configuration is $^2A''$, i.e., $(1A')^2\ (2A')^2\ (1A'')^2\ (3A')^2\ (4A')^2\ (2A'')^2\ (5A')^2\ (3A'')^2\ (6A')^2\ (4A'')^2\ (7A')^2\ (5A'')^2\ (8A')^2\ (9A')^2\ (6A'')^2\ (10A')^2\ (11A')^2\ (12A')^2\ (7A'')^2\ (13A')^2\ (8A''\uparrow)^1$; for anionic Y_3O^-, the configuration is $^3A''$, i.e., $(1A')^2\ (2A')^2\ (3A')^2\ (1A'')^2\ (4A')^2\ (2A'')^2\ (5A')^2\ (6A')^2\ (7A')^2\ (3A'')^2\ (4A'')^2\ (8A')^2\ (5A'')^2\ (9A')^2\ (6A'')^2\ (10A')^2\ (11A')^2\ (12A')^2\ (7A'')^2\ (13A')^2\ (8A''\uparrow)^1\ (14A'\uparrow)^1$; for cationic Y_3O^+, the configuration is $^1A'$, i.e., $(1A')^2\ (2A')^2\ (1A'')^2\ (3A')^2\ (4A')^2\ (2A'')^2\ (5A')^2\ (6A')^2\ (7A')^2\ (3A'')^2\ (8A')^2\ (4A'')^2\ (5A'')^2\ (9A')^2\ (10A')^2\ (6A'')^2\ (11A')^2\ (12A')^2\ (13A')^2\ (7A'')^2$.

Table 2 lists the adiabatic and vertical electron affinities (EAs) and ionization potentials (IPs) for Y_3O. Two types of vertical EAs and IPs are defined as follows: in type I, the total energy differences of the neutral molecule and ions are calculated at the optimized molecular geometry; and in type II, they are calculated at the optimized ionic geometry. The vertical EAs and IPs are corresponding to the different experimental processes. For example, the EA_{verII} is corresponding to the measured EA in PES of anions, and the IP_{verI} is corresponding to the measured IP in PES of cations. Our calculated EA_{ad}(1.22 eV), EA_{verII}(1.33 eV) and IP_{verI}(4.84 eV) are in good agreement with experimental value (1.10 ± 0.19) eV [6], (1.33 ± 0.8) eV [6] and 4.92 eV [4], respectively. The calculated

Table 2. The adiabatic and vertical electron affinities (EAs) (in eV) and ionization potential (IPs) (in eV)) for the Y_3O.

	adiabatic (eV)	vertical I (eV)	vertical II (eV)
EA	1.22	1.13	1.33
IP	4.71	4.84	4.49

Table 3. Mulliken charges and total atomic spin densities.

		O_1	Y_2	Y_3	Y_4	sum
Y_3O	charge	−0.823	0.264	0.264	0.295	0
	net spin	−0.021	0.367	0.367	0.287	1
Y_3O^-	charge	−0.861	−0.045	−0.045	−0.049	−1
	net spin	−0.037	0.681	0.681	0.675	2
Y_3O^+	charge	−0.817	0.604	0.604	0.609	+1
	net spin	−0.021	0.560	0.560	0.900	2

EAs and IPs have the following energy orders as usual: $EA_{verI} < EA_{ad} < EA_{verII}$, and $IP_{verII} < IP_{ad} < IP_{verI}$.

Since the LANL2DZ basis set does not contain polarization functions for oxygen atom, whether polarization functions have effect on the calculation result is a question. In order to check the effect of polarization functions on EAs and IPs for Y_3O clusters, the polarized basis set D95* for O and LANL2DZ basis set for Y are used. Then our calculated EA_{ad}, EA_{verII} and IP_{verI} are 1.27 eV, 1.34 eV and, 4.90 eV, respectively. Moreover, with the diffused and polarized basis set 6-311+G* for O and LANL2DZ basis set for Y, the EA_{ad}, EA_{verII} and IP_{verI} are 1.18 eV, 1.32 eV and 4.92 eV, respectively. Apparently, the calculated results with both kinds of basis sets are almost the same as the foregoing calculations. It is evident that the effect of the diffuse and polarization functions for the oxygen atom is neglectable.

The Mulliken charge and spin populations of Y_3O and its ions are presented in Table 3. It is clear that the additional electron of the Y_3O^- is mainly located on the three yttrium atoms, while the lost electron of the Y_3O^+ mainly comes from the three yttrium atoms, and the charges on the oxygen atoms of all three clusters are almost the same. The analysis of the spin density for ions of Y_3O shows that the unpaired electrons are mainly localized on the Y_3 fragment. Table 4 lists the *s*-, *p*-, and *d*-gross atomic orbital populations (GAOPs) for the Y_3O, Y_3O^-, Y_3O^+. The GAOPs show, that the additive electron of Y_3O^- mainly distributes to the $5p$ orbitals of the three yttrium atoms, while the lost electron of Y_3O^+ mainly comes from $5s$ orbitals of the three yttrium atoms.

3.2 Analysis of PES data

Pramann et al. [6] presented the PES of Y_3O but did not assign the features in the PES which correspond to the transitions from the anion to the neutral molecule with the detachment of an electron. Here we present a theoretical assignment.

First, we assume that with the detachment of an electron, the transitions from Y_3O^- to Y_3O are vertical. This means that neutral Y_3O here should keep the same geometry as Y_3O^-. Secondly, we assume that all the detachment features are only corresponding to the electronic transitions from the anion ground state to the neutral molecule. That means that the possible transitions due to the excited states of the anion would not be considered. The neutral Y_3O and the detached electron can be viewed as a system whose total spin should be equal to that of Y_3O^-. Removing an electron from the triplet state of the anion can result in a doublet or a quadruplet state for the neutral molecule.

Table 4. The gross atomic orbital populations of the Y_3O, Y_3O^-, Y_3O^+ at their equilibrium geometries and the Y_3O at anionic equilibrium geometry (Y_3O(A)).

atomic orbital		gross orbital populations			
		Y_3O^+	Y_3O	Y_3O(A)	Y_3O^-
O_1	$1s$	1.999	1.999	1.999	1.999
	$2s$	1.879	1.879	1.879	1.880
	$2p$	4.940	4.945	4.953	4.969
Y_2	$4s$	1.987	1.986	1.986	1.987
	$4p$	5.985	5.987	5.987	5.988
	$4d$	1.174	1.035	1.018	1.097
	$5s$	1.175	1.601	1.633	1.622
	$5p$	0.077	0.126	0.106	0.359
Y_3	$4s$	1.987	1.986	1.986	1.987
	$4p$	5.985	5.987	5.987	5.988
	$4d$	1.174	1.035	1.018	1.097
	$5s$	1.175	1.602	1.633	1.622
	$5p$	0.076	0.126	0.106	0.359
Y_4	$4s$	1.987	1.986	1.986	1.987
	$4p$	5.983	5.985	5.985	5.985
	$4d$	1.351	1.162	1.155	1.230
	$5s$	0.847	1.386	1.406	1.395
	$5p$	0.223	0.187	0.177	0.451

At the equilibrium geometry of the anion, the ground state of the Y_3O is as $^2A''$, which is the same as that in the equilibrium geometry of itself. And the lowest quadruplet is $^4A''$, i.e., $(1A')^2$ $(2A')^2$ $(1A'')^2$ $(3A')^2$ $(4A')^2$ $(2A'')^2$ $(5A')^2$ $(6A')^2$ $(3A'')^2$ $(7A')^2$ $(4A'')^2$ $(8A')^2$ $(5A'')^2$ $(9A')^2$ $(10A')^2$ $(6A'')^2$ $(11A')^2$ $(12A')^2$ $(7A'')^2$ $(13A'\uparrow)^1$ $(8A''\uparrow)^1$ $(14A'\uparrow)^1$. Our calculation shows that the energy of the latter is 0.23 eV higher than that of the former.

We calculate the excitation energies of the neutral Y_3O at the equilibrium geometry of the anion via TDDFT. The first 11 excited doublets and the first 6 excited quadruplets with the binding energy lower than 2.10 eV are listed in Tables 5 and 6, respectively. Because the excitation energies of excited doublet and quadruplet states are relative to the energies of the $^2A''$ and $^4A''$ states, respectively, it is necessary to correlate these excited states to the states in the PES of Y_3O^-. The X state in the experimental PES should be determined first. Since the X state is usually believed to be corresponding to the transition from the ground state of the anion to the ground state of the

Table 5. The calculated excitation energies (Ei) for the doublet of Y_3O at anionic equilibrium geometry and binding energies (BEs) in PES of Y_3O^-.

state	dominant component	E (eV)	BE IN PES (eV)	
			Ei + EAexp	Exp [6]
0		0.0	1.330	1.33
1	$6A'' \downarrow \rightarrow 14A' \downarrow$	0.134	1.464	
2	$6A'' \uparrow \rightarrow 16A' \uparrow$, $6A'' \downarrow \rightarrow 14A' \downarrow$	0.221	1.551	
3	$8A'' \uparrow \rightarrow 9A'' \uparrow$	0.278	1.608	
4	$8A'' \uparrow \rightarrow 10A'' \uparrow$	0.294	1.624	1.65
5	$7A'' \downarrow \rightarrow 14A' \downarrow$	0.437	1.767	
6	$7A'' \uparrow \rightarrow 15A' \uparrow$	0.451	1.781	1.80
7	$13A' \uparrow \rightarrow 14A' \uparrow$	0.528	1.858	
8	$7A'' \downarrow \rightarrow 14A' \downarrow$	0.576	1.906	
9	$7A'' \downarrow \rightarrow 16A' \downarrow$	0.748	2.078	2.05
10	$8A'' \uparrow \rightarrow 11A'' \uparrow$	0.764	2.094	
11	$8A'' \uparrow \rightarrow 17A' \uparrow$	0.771	2.101	

A $\rightarrow$ B denotes a singly excited determinant which is formed by replacing the occupied orbital A with the virtual orbital B in the $^2A''$ state determinant.

Table 6. The calculated excitation energies (Ei) for the quadlet of Y_3O at anionic equilibrium geometry and binding energies (BEs) in PES of Y_3O^-.

state	dominant component	Ei (eV)	BE IN PES (eV)	
			Ei + ΔE + EAexp	Exp [6]
0		0.000	1.560	
1	$7A'' \downarrow \rightarrow 13A' \downarrow$	0.089	1.649	1.65
2	$14A' \uparrow \rightarrow 16A' \uparrow$	0.109	1.669	
3	$8A'' \uparrow \rightarrow 16A' \uparrow$	0.128	1.688	1.70
4	$14A' \uparrow \rightarrow 15A' \uparrow$	0.358	1.918	
5	$14A' \uparrow \rightarrow 9A'' \uparrow$	0.378	1.938	
6	$8A'' \uparrow \rightarrow 9A'' \uparrow$	0.536	2.096	2.05

A $\rightarrow$ B denotes a singly excited determinant which is formed by replacing the occupied orbital A with the virtual orbital B in the $^4A''$ state determinate. $\Delta E = 0.23$ eV.

neutral molecule at the anionic geometry, so the binding energy of X state is the vertical electron affinity of the molecule (EA_{verII}).

With the X state, we can transform the excitation energies of the doublets to the binding energies (BEs) in the PES by adding the vertical EA. In general, in order to avoid the effect of the deviation of calculated EA, the experiment EA, 1.33 eV, is used (in Tab. 5). For the quadruplets, both the vertical EA and the energy difference between the $^2A''$ and $^4A''$ states, 0.23 eV, should be added (in Tab. 6).

In fact each of the broad files in experiment PES is ascribable to a series of excited energy levels and vibrational energy levels, and we could only assign a certain excited state to the binding energy location of the corresponding peak for the PES in Tables 5 and 6. Therefore, the discrete excited energies should be extended to a continuous spectrum to compare with the main features of PES. The strength of the peak of PES is determined by two factors: one is the density of excited states, and the other is the transition dipole between the initial state and the final state. But in our calculations only the influence of the density of excited states is considered.

Figure 2 shows our calculated spectrum. Here we perform a Lorentzian extension of BEs and sum them over to obtain the calculated photoelectron spectrum. Compared with the experimental PES [6], four distinct spectral features at X, A, B, C in Figure 2 are discussed as follows. The peaks X and A with binding energies 1.33 and 1.67 eV are just corresponding to the structures X and A of the experimental PES [6], respectively.The calculated value for the peak A is in the experimental range of 1.60−1.70 eV. The peak C with the calculated binding energy 1.92 eV is corresponding to the small peak at 2.05 eV in the deep valley of the experimental PES [6]. In addition, the small peak B of 1.78 eV is exactly corresponding to a small peak on the right hand side shoulder of the experimental peak A. The existence of the strength difference between experimental and calculated spectrum is due to the fact that we have neglected the influence of the transition dipole

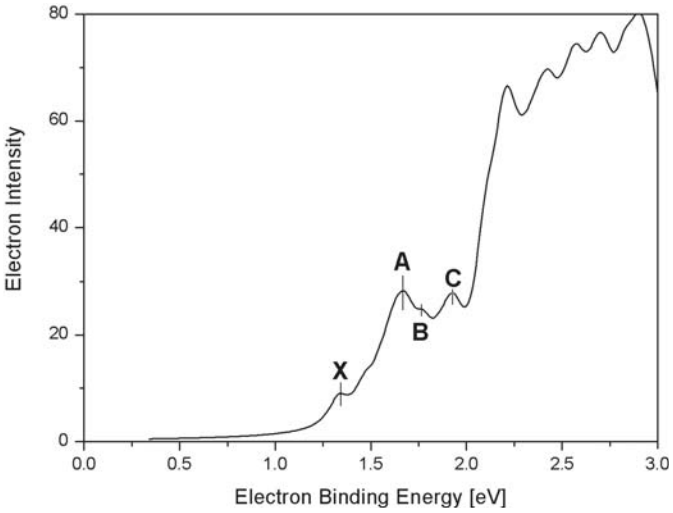

Fig. 2. The calculated photoelectron spectrum of Y_3O^-.

as mentioned before. As far as the complicated structure above 2.1 eV in the experimental PES we could not give an explicit assignment. Because there are too many peaks to be distinguished with each in the PES and the accurate excited energy for higher excited states could not be easily obtained via the calculation.

Apparently, the calculated spectrum is in good agreement with the main features of the experimental one [6].

4 Summary

In this paper, we have reported a comprehensive study on the structural, electronic properties of Y_3O cluster in its neutral, anionic, and cationic charge states using the first-principles DFT at the B3LYP level. The equilibrium geometries and electronic configurations of the neutral molecule and its ions are obtained. All the equilibrium geometries of Y_3O, Y_3O^-, and Y_3O^+ are three-dimensional with C_S symmetries. The ground states of Y_3O, Y_3O^-, and Y_3O^+ are the doublet ($^2A''$), triplet ($^3A''$) and singlet ($^1A'$), respectively. The Mulliken charge and spin populations of Y_3O molecule and its ions are discussed. A theoretical assignment at the B3LYP level for the features in the PES is performed. The calculated spectrum is in good agreement with the available experimental data. All the results obtained here confirm that the most stable geometries of the neutral and ionic Y_3O clusters are three-dimensional structures with the C_S symmetry.

This work was partially supported by the National Project for the Development of Key Fundamental Sciences in China (G1999075305), by the National Natural Science Foundation of China (20025309, 50121202), by the Foundation of Ministry of Education of China, and by the Foundation of the Chinese Academy of Science.

References

1. A.W. Castleman Jr, K.H. Bowen Jr, J. Phys. Chem. **100**, 12911 (1996)
2. V.E. Henrich, P.A. Cox, *the Surface Science of Metal Oxides* (Cambridge University Press, New York, 1994)
3. C.N.R. Rao, Annu. Rev. Phys. Chem. **40**, 291 (1989)
4. M. Knickelbein, J. Chem. Phys. **102**, 1 (1995)
5. H. Wu, L. Wang, J. Phys. Chem. A **102**, 9129 (1998)
6. A. Pramann, Y. Nakamura, A. Nakajima, J. Phys. Chem. A **105**, 7534 (2001)
7. R.E. Stratmann, G.E. Scuseria, M.J. Frisch, J. Chem. Phys. **109**, 8218 (1998)
8. J.B. Foresman, M. Head-Gordon, J.A. Pople, M.J. Frisch, J. Phys. Chem. **96**, 135 (1992)
9. E. Broclawik, T. Borowski, Chem. Phys. Lett. **339**, 433 (2001)
10. B. Dai, K. Deng, J. Yang, Q. Zhu, J. Chem. Phys. **118**, 9608 (2003)
11. B. Dai, K. Deng, J. Yang, Chem. Phys. Lett. **364**, 188 (2002)
12. M.J. Frisch et al., *Gaussian 98*, Gaussian Inc., Pittsburgh, PA, USA
13. A.D. Becke, J. Chem. Phys. **98**, 5648 (1993)
14. F.S. Legge, G.L. Nyberg, J.B. Peel, J. Phys. Chem. A **105**, 7905 (2001)
15. S.M.E. Green, S. Alex, N.L. Fleischer, E.L. Milliam, T.P. Marcy, D.G. Leopold, J. Chem. Phys. **114**, 2653 (2001)